



HHS Public Access

Author manuscript

J Am Chem Soc. Author manuscript; available in PMC 2025 May 21.

Published in final edited form as:

J Am Chem Soc. 2025 March 26; 147(12): 10382–10390. doi:10.1021/jacs.4c17657.

Photoredox/Pyridine *N*-Oxide Catalyzed Carbohydroxylation and Aminohydroxylation of α -Olefins

Cristina Ascenzi Pettenuzzo,

Department of Chemistry and Chemical Biology, Indiana University Indianapolis, Indianapolis, Indiana 46202, United States

Deepak Ranjan Pradhan,

Department of Chemistry, Binghamton University, Binghamton, New York 13902, United States

Jujhar Singh,

Department of Chemistry and Chemical Biology, Indiana University Indianapolis, Indianapolis, Indiana 46202, United States

Lichuan Liu,

Department of Chemistry and Chemical Biology, Indiana University Indianapolis, Indianapolis, Indiana 46202, United States

Gabe Cuffel,

Department of Chemistry and Chemical Biology, Indiana University Indianapolis, Indianapolis, Indiana 46202, United States

Mathew J. Vetticatt,

Department of Chemistry, Binghamton University, Binghamton, New York 13902, United States

Yongming Deng

Department of Chemistry and Chemical Biology, Indiana University Indianapolis, Indianapolis, Indiana 46202, United States

Abstract

Regioselective carbohydroxylation and aminohydroxylation of α -olefins were developed by a photoredox catalyst and pyridine *N*-oxide. This approach offers the catalytic and direct conversion of unactivated alkenes to a series of primary alcohols, including those bearing β -quaternary

Corresponding Authors Mathew J. Vetticatt – Department of Chemistry, Binghamton University, Binghamton, New York 13902, United States; vetticatt@binghamton.edu; **Yongming Deng** – Department of Chemistry and Chemical Biology, Indiana University Indianapolis, Indianapolis, Indiana 46202, United States; yongdeng@iu.edu.

Supporting Information

The Supporting Information is available free of charge at <https://pubs.acs.org/doi/10.1021/jacs.4c17657>.

Details of experimental procedures, mechanistic studies, and spectroscopic data for the products, NMR spectral data, and single-crystal X-ray data of compound **14** (PDF)

Accession Codes

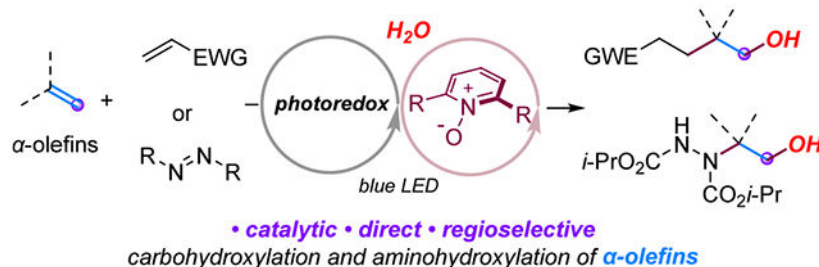
Deposition Number 2355768 contains the supplementary crystallographic data for this paper. These data can be obtained free of charge via the joint Cambridge Crystallographic Data Centre (CCDC) and Fachinformationszentrum Karlsruhe Access Structures service.

Notes

The authors declare no competing financial interest.

carbon centers and β -amino alcohols. The regioselective difunctionalization is enabled by the radical addition of α -olefin from the pyridine *N*-oxy radical, which is generated from readily available pyridine *N*-oxide via photoredox catalyzed single-electron oxidation. A combination of experimental and computational mechanistic studies was employed to lend support for the proposed reaction mechanism that proceeds via interwoven radical steps and polar substitution. The implications of this method for regioselective difunctionalization of α -olefins were further demonstrated by the examples of carboetherification, carboesterification, and lactone formation.

Graphical Abstract



1. INTRODUCTION

Primary alcohols are one of the fundamental substrates in organic chemistry, and they have broad usefulness in pharmaceutical, agrochemical, and bulk/fine chemical industries.¹ Their synthesis from terminal alkenes via regioselective (anti-Markovnikov) hydration represents a direct and compelling synthetic route using abundantly available substrates.² Primary aliphatic alcohols are commonly accessed through a two-step redox process (Figure 1A). For instance, the two-step hydroboration-oxidation sequence is a robust and widely applied approach to achieve anti-Markovnikov hydration of alkenes.³ In industry, the Ziegler process and hydroformylation/hydrogenation prevail in producing primary alcohols.⁴ In addition, the synthesis of primary alcohols has been reported by transition metal-catalyzed regioselective hydrogenation of epoxides.⁵ However, these transformations generally require stoichiometric oxidation/reduction and multistep operations. To address these challenges, tremendous efforts have been made in developing direct and catalytic production of primary alcohols from olefins and water through transition metal catalysis and photoredox catalysis.⁶ The Grubbs group demonstrated a triple relay catalysis system for one-pot anti-Markovnikov hydration of styrenes with water (Figure 1B).⁷ A photoredox approach was reported by the Lei group using an acridinium photocatalyst that enables the single-electron oxidation of styrenes and multisubstituted alkenes to achieve the synthesis of primary alcohols (Figure 1B).⁸ Despite these significant achievements, the reported catalytic approaches to primary alcohols share the common limitations to styrenes or multisubstituted olefin substrates. For example, α -olefins are beyond the scope of anti-Markovnikov hydration in modern photoredox chemistry due to their challenging single-electron oxidation.^{6b}

The radical addition of unsymmetrical olefins represents an alternative powerful strategy for regioselective (anti-Markovnikov) construction of the carbon-heteroatom bond at the less-substituted carbon of alkene. Although impressive nitrogen,⁹ sulfur,¹⁰ and halide-

centered¹¹ radical-mediated catalytic anti-Markovnikov addition reactions of unactivated olefins were developed, the corresponding oxygen-centered radical-mediated reactions remain elusive. Recently, seminal work from Han et al.,¹² Ready and Leng,¹³ and Glorius et al.,¹⁴ respectively, demonstrated photoredox-catalyzed oxygen-centered radical mediated anti-Markovnikov hydroxylation of unactivated olefins (Figure 1C). These methodologies provide evidence for applying oxy radicals in the regioselective addition of unactivated alkenes. However, substrate prefunctionalization and employment of stoichiometric oxygen radical precursors were required in these protocols.

Recently, our group and others have reported a photocatalytic strategy for pyridine *N*-oxy radical generation through single-electron oxidation of pyridine *N*-oxides.¹⁵ This strategy has been explored in the development of various radical cascade reactions and C—H functionalizations.¹⁵ In view of the body of literature on alkene addition by oxy radicals and the versatile reactivity of pyridine *N*-oxy radicals, we hypothesized that the photocatalytically generated electrophilic pyridine *N*-oxy radicals might initiate the regioselective addition of α -olefins at the terminal carbons in accordance with the persistent radical effect and favored polarity matching (Figure 2). The resulting more stable carbon radical intermediate can undergo a Giese-type reaction with an electrodeficient alkene to generate an *N*-alkoxy-pyridinium intermediate. We proposed that the *N*-alkoxy-pyridinium intermediate might react with water through substitution to furnish the primary alcohol product, achieving regioselective carbohydroxylation. Herein, we report an organophotoredox/pyridine *N*-oxide catalyzed regioselective carbohydroxylation and aminohydroxylation of α -olefins (Figure 2). The carbohydroxylation successfully delivered a series of primary alcohols, including those bearing β -quaternary carbon centers and medicinally relevant pyridine cores. Additionally, the examples of aminohydroxylation provided a new method for the production of β -amino alcohols. These results point the way to a catalytic and direct approach with modular control of regioselectivity for the difunctionalization of α -olefins by a dual photoredox/pyridine *N*-oxide catalytic system via interwoven radical steps and polar substitution.

2. RESULTS AND DISCUSSION

2.1. Development and Optimization.

To test the principle, a proposed carbohydroxylation of 1-hexene with benzalmalononitrile as the radical trapping agent and water as the nucleophile was chosen as the model reaction (Figure 3A). Based on our and others' previous studies, 9-mesityl-10-methylacridinium (Mes-Acr-MeClO₄, **PC1**, $E_{1/2}^{\text{red}*} = +2.06$ V vs SCE) was first examined as the photoredox catalyst to initiate the photoinduced single-electron oxidation of pyridine *N*-oxides for the generation of *N*-oxy radicals.^{6b,15} Meanwhile, the selection of 1-hexene as the model α -olefin substrate is based on its high oxidation potential ($E_{1/2}^{\text{ox}} > +2.50$ V vs SCE),¹⁶ which is outside of the oxidation range of the acridinium excited state. We started our investigation with a survey of pyridine *N*-oxides by the reaction of 1-hexene with benzalmalononitrile **PC1** under irradiation with a blue LED light in acetonitrile/water (10:1) (Figure 3A).

In line with our hypothesis, when 20 mol % pyridine *N*-oxide (**1a**) was applied, the desired carbohydroxylation product **2** (*d.r.* = 1:1) was obtained in 14% yield with exclusive

regioselectivity, and unreacted radical acceptor was recovered (Figure 3A, entry 1). However, along with the formation of primary alcohol **2**, an *ortho*-alkylation product **3** (13%) was generated from the reaction of **1a** (Figure 3B). Based on Miura et al.'s report on photocatalyzed *ortho*-alkylation of pyridine *N*-oxides,¹⁷ the formation of **3** is rationalized via an intramolecular radical *ortho*-addition followed by β -N—O and β -C—C bonds scissions with losing formaldehyde fragment.¹⁷ To suppress the competing *ortho*-alkylation, *ortho*-disubstituted *N*-oxides **1b–1e** (entries 2–6) were screened. 2,6-Dichloropyridine *N*-oxide **1b** was the most efficient for the desired carbohydroxylation (entry 2). It is worth mentioning that when 2,6-dibromopyridine *N*-oxide **1d** was applied, the allylic alkylation product **4** of 1-hexene with benzalmalononitrile was obtained in 34% yield (**4**, Figure 3C). Compound **4** is formed through allylic C—H functionalization with **1d** as an H atom transfer (HAT) agent, while the alkylation product was not detected when **1b** was examined.¹⁸

Following the promising results, extensive condition optimizations, including surveys of photocatalysts, solvents, and additives, were performed (see Tables S1–S4 in the Supporting Information). Mes-(^tBu)₂Acr-PhBF₄ (**PC2**, $E_{1/2}^{\text{red}*} = +2.15$ V vs SCE)^{6b,19} proved to be the most efficient photocatalyst (entry 7). Upon solvent screening, acetone was identified as the optimized solvent (entry 8). The necessity of water in achieving the desired carbohydroxylation was validated by a control experiment (entry 9). In consideration of the proton transfer sequence (Figure 2), various acid additives were examined (entries 10–14 and Table S3). The highest reaction efficiency was obtained when acetone was applied as a solvent with the addition of 2.0 equiv of trichloroacetic acid (TFA) (entry 11). In addition to presumably facilitating proton transfer, TFA is also found to promote the nucleophilic substitution step. It occurs through hydrogen bonding formations between trifluoroacetate, *N*-alkoxyppyridinium intermediate, and water. This process is discussed in more detail in a later section by computational modeling of the reaction.

Encouragingly, as shown in Figure 3D, when the reaction of 2-ethyl-1-butene ($E_{1/2}^{\text{ox}} = +2.43$ V vs SCE) was subjected to 20 mol % **1b** in the presence of **PC2** and TFA in acetone/water under blue light irradiation (condition A), the primary alcohol product **5** was obtained in high isolated yield (82%) with exclusive regioselectivity. Considering the ready availability of pyridine *N*-oxides, the loading of **1b** was increased to 50 mol % in the reaction of 1-hexene, and **2** can be produced in satisfactory yield (74%, entry 15 and Figure 3D, condition B). In the absence of pyridine *N*-oxide, the control reaction of 1-hexene, benzalmalononitrile, and water, solely catalyzed by the photocatalyst under blue light, did not participate in the proposed carbohydroxylation, and unreacted substrates were recovered (entry 18). This result aligns with reports from Nicewicz and others that α -olefins are generally nonoxidizable by the acridinium excited state.^{8,10f,16,18} Omitting the photocatalyst or the performance of the reaction in the dark leads to no reaction, revealing its crucial role (entries 19 and 20).

2.2. Reaction Scope.

On the basis of this knowledge of the optimized reaction, substrate generality was investigated. We first examined electron-deficient alkenes as radical acceptors in the regioselective carbohydroxylation of 2-ethyl-1-butene (condition A) and 1-hexene

(condition B). Various electron-deficient alkenes, including vinylpyridines, vinylpyrazine, *tert*-butyl methacrylate, and α -(trifluoromethyl)styrene, reacted smoothly, generating the corresponding primary alcohols in good to moderate yields (Figure 4, **6–12**). In the cases of vinylpyridines, it is presumed that they were protonated by TFA, becoming more electrophilic to facilitate the Giese radical addition. 4-Vinylpyridine was found to be less reactive than 2-vinylpyridine, producing **8** in 58% yield.

With regard to the omnipresence of the pyridine scaffold in pharmaceuticals, agrochemicals, and natural products, we then conducted a study of the scope of α -olefins using 2-vinylpyridine as the radical acceptor. Generally, β , β -disubstituted α -olefins (condition A) exhibited higher reactivity than monosubstituted α -olefins (condition B). 2-Methyl-1-pentene underwent efficient regioselective carbohydroxylation (**13**). Exomethylene containing 4-methylene-1-tosylpiperidine reacted successfully to generate **14** in 75% yield. The structure of primary alcohol product **14** was identified spectroscopically and confirmed by X-ray diffraction analysis.²⁰

Furthermore, we evaluated α -olefins with various functional groups (**15–20**). Olefins containing ketones, esters, nitrile, and chloro-substituent were compatible with this reaction, affording primary alcohols in good to moderate yields (**15–19**). However, bromo-substituted alkene furnished the desired product **20** in low yield (32% yield) even with 50 mol % *N*-oxide loading. In addition to terminal olefins, internal and cyclic alkenes (**21–25**) were carbohydroxylated to give the corresponding alcohol products in moderate reaction yields with low diastereoselectivities. The alcohol product generated from dimethyl hex-3-enedioate underwent intramolecular transesterification, delivering lactone product **26** in 36% yield. Notably, camphene was a good substrate for this transformation, giving the carbohydroxylation product **27** in 71% yield with a stereoselectivity ratio of 10:1. Moreover, this protocol can be applied to a terminal alkene tethered Ibuprofen derivative (**28**). Indeed, our current method exhibits certain substrate limitations. Our attempts on alkenals and unprotected olefinic amines did not yield the desired primary alcohol products. The method presented here for regioselective carbohydroxylation allows the generation of various primary alcohols from unactivated α -olefins and water directly. Remarkably, it provides a direct approach to the synthesis of primary alcohols containing β -quaternary carbon centers.

In order to further explore the synthetic potential of the photoredox-catalyzed regioselective difunctionalization of α -olefins, we next applied this protocol to the aminohydroxylation of α -olefins (Figure 5). Diisopropyl azodicarboxylate (DIAD) was utilized as the carbon radical trapping agent. Gratifyingly, upon employing 50 mol % **1b** and acridinium photocatalyst (condition B), the desired aminohydroxylation products were successfully produced from various α -olefins in acceptable to good yields (**26–31**). In addition to α -olefins, internal alkenes, e.g., cyclohexene, were examined under the photocatalytic condition. However, the allylic C—H amination product of cyclohexene **35** (46%) was obtained as the major reaction outcome, with the generation of the desired alcohol product in low yield. The synthetic usefulness of the aminohydroxylation products was then exemplified by preparing the hydrazide-containing oxazolidin-2-one **37** from base-promoted cyclization of **29** (Figure 5b). Following established procedures,²¹ the subsequent reaction of

37 with methyl bromoacetate in the presence of cesium carbonate gave the oxazolidinone **38** via the nitrogen–nitrogen bond cleavage.

2.3. Mechanistic Studies.

Previous studies from our group and others have demonstrated the photoredox-catalyzed generation of pyridine *N*-oxy radicals through single-electron oxidation from pyridine *N*-oxides. It was further validated by the fluorescence quenching experiments and electrochemical studies of an acridinium photocatalyst, 2,6-dichloropyridine *N*-oxide, and α -olefins (Figure 6A). The Stern–Volmer fluorescence quenching analysis determined that the light-excited photocatalyst Mes-(^tBu)₂Ac⁺* was quenched by 2,6-dichloropyridine *N*-oxide (**1b**, $K_{sv} = 34.2$) rather than α -olefin or benzalmalononitrile. It is consistent with our electrochemical studies that the excited photocatalyst Mes-(^tBu)₂Ac⁺* ($E_{red}^* = 2.15$ V vs SCE) oxidizes **1b** ($E_{1/2}^{ox} = +2.06$ V vs SCE) via photoinduced single-electron oxidation. As documented, α -olefins (e.g., 1-hexene: $E_{1/2}^{ox} > +2.50$ V vs SCE; 2-ethyl-1-butene: $E_{1/2}^{ox} = +2.43$ V vs SCE) are outside of the oxidation range of the acridinium excited state, which excludes the pathway of alkene cation radical generation from α -olefins. Furthermore, the generation of a carbon radical upon alkene addition by *N*-oxy radical addition was evidenced by the cyclization/carbohydroxylation of 1,6-heptadiene (Figure 6B). The disubstituted cyclopentane **32** was obtained in 52% yield and was afforded through an intramolecular radical addition to the pendant alkene.

As outlined in our research design (Figure 2B), it is proposed that upon the Giese-type reaction the resulting *N*-alkoxy-pyridinium intermediate undergoes nucleophilic substitution with water to yield the alcohol product and regenerates pyridine *N*-oxide. Early reports from Katritzky and Lunt provided evidence for the reactivity of *N*-alkoxy-pyridinium salt in nucleophilic substitution reactions and pyridine *N*-oxide regeneration.²² Another possible pathway involving reductive cleavage of the N–O bond in *N*-alkoxy-pyridinium may lead to alcohol product generation.²³ However, the use of a catalytic amount of **1b** in producing the alcohol products suggests regeneration of *N*-oxide. To reveal the origin of the hydroxyl group in the product and elucidate the mechanism, an isotopic labeling experiment using H₂¹⁸O (95 atom % ¹⁸O) as the nucleophile was performed for carbohydroxylation of 2-ethyl-1-butene (Figure 6C). Under the optimized reaction conditions (condition A), the primary alcohol product was obtained in 78% yield with ¹⁸O/¹⁶O = 92/8. This result demonstrates the nucleophilic substitution step of *N*-alkoxy-pyridinium with water for alcohol production, and the achieved catalytic use of **1b** further validates our hypothesis.

In view of the feasibility of the nucleophilic substitution step, we envisioned that the scope of nucleophiles could be extended, e.g., alcohols and carboxylates for carboxylation. As predicted, the carboetherification product **33** could be obtained in 42% yield when *tert*-butanol was employed under the photoredox/pyridine *N*-oxide condition (Figure 6D). The use of acetic acid as the nucleophile was also attempted. With a brief condition screening, the desired regioselective carboesterification product **34** was yielded in 56% with excess acetic acid (10.0 equiv) in the presence of 2,6-lutidine (5.0 equiv). It is worth noting that the use of the buffer system of acetate and acetic acid is important to receive the observed reactivity of carboesterification. It is presumed that the addition of the

base is to deprotonate acetic acid in producing acetate to facilitate the substitution step. Moreover, we predicted that a regioselective lactonization of olefinic carboxylic acid could be achieved via the developed radical addition and polar substitution sequences. As shown in Figure 6D, γ -substituted δ -lactone **35** was successfully yielded from 4-pentenoic acid through photoredox/pyridine *N*-oxide catalyzed radical addition/cyclization. Although the unoptimized conditions produced **33–35** in moderate yields, these results provide a proof of principle for the photoredox/pyridine *N*-oxide protocol in the development of regioselective difunctionalization of α -olefins and heterocycle synthesis.

To provide more insight into the mechanistic understanding, we performed DFT calculations to evaluate the feasibility of our proposed mechanism. We modeled the reaction of 2-ethyl-1-butene and benzalmalonitrile catalyzed by **PC2** and **1b** using B3LYP-D3(BJ)/6-31+G*²⁴PCM²⁵(acetone) calculations as executed in Gaussian '16.²⁶ The results of our DFT evaluation of the free energy profile of the catalytic cycle including the SET steps are shown in Figure 7. Based on the experimentally determined redox potentials of **PC2** and **1b**, we estimate that the initial SET from **1b** to **PC2** is thermodynamically favored by ~ 0.7 kcal/mol.²⁷ The resulting *N*-oxy radical (**1b**[•]) undergoes facile addition to 2-ethyl-1-butene (Figure 7, TS_{C-O} , $G^\ddagger = 0.7$ kcal/mol) resulting in the tertiary carbon-centered radical (*Int1*).²⁸ The next step in the catalytic cycle involves the Giese-type addition of benzalmalonitrile to *Int1* (Figure 7, TS_{C-C} , $G^\ddagger = 17.8$ kcal/mol), which is rendered irreversible by a rapid SET from the reduced **PC2** ($G = -18.1$ kcal/mol) to the Giese-adduct (*Int2*). The resulting carbanion intermediate (*Int3*) is rapidly protonated (Figure 7, TS_{Prot} , $G^\ddagger = 3.7$ kcal/mol) by trifluoroacetic acid to form the *N*-alkoxy pyridinium trifluoroacetate intermediate (*Int4*). Finally, we modeled the substitution of pyridine *N*-oxide from the *N*-alkoxy pyridinium intermediate by water. In the lowest energy transition state for this step, water is activated by the trifluoroacetate counterion, which is dually H-bonded to water, and the C—H of the carbon that is attached to the *N*-alkoxy pyridinium leaving group (Figure 7, TS_{Sub}). This step is the rate-determining step in our computed free energy profile with a free energy barrier of 24.3 kcal/mol, which is reasonable for a reaction that proceeds at 45 °C.²⁹ These data substantiate the important role of trifluoroacetic acid in enhancing reaction efficiency. Integrating experimental and computational data supports a plausible mechanism for photoredox/pyridine *N*-oxide catalyzed regioselective difunctionalization of α -olefins, involving interwoven radical steps and polar substitution.

3. CONCLUSIONS

In summary, we have developed a direct and catalytic strategy for the regioselective carbohydroxylation of α -olefins via pyridine *N*-oxide/photoredox catalysis. The demonstrated concept was extended to the regioselective aminohydroxylation of unactivated olefins with azodicarboxylates. Various α -olefins were successfully functionalized in producing diverse functional-group-rich primary alcohols, showcasing the practicality, generality, and robustness of the present method. The mechanistic insights from experimental and computational studies reported herein highlight the centrality of interwoven radical and polar steps by photoredox/pyridine *N*-oxide catalysis in regioselective difunctionalization of α -olefins. We anticipate that an improved understanding of the reactivity and selectivity of pyridine *N*-oxy radicals will provide further opportunities

for catalyst optimization that support the ongoing expansion of alkene functionalization classes. For example, this may allow us to approach the enduring challenge of the anti-Markovnikov hydration of α -olefins and apply this strategy in new synthetic contexts.

Supplementary Material

Refer to Web version on PubMed Central for supplementary material.

ACKNOWLEDGMENTS

Research reported in this publication was supported by the American Chemical Society Petroleum Research Fund under PRF 66112-ND1 (Y.D.), the National Institutes of Health (NIGMS) under R35 GM150542 (Y.D.), and R35 GM145320 (M.J.V.). J.S. acknowledges financial support from the Beckman Scholars Program. The computational calculations were performed with an expanse cluster at the San Diego Supercomputer Center through allocation CHE240143 from the Advanced Cyberinfrastructure Coordination Ecosystem: Services & Support (ACCESS) program, which is supported by U.S. National Science Foundation grants #2138259, #2138286, #2138307, #2137603, and #2138296. Y.D. acknowledges Dr. Ian Webb for assistance in ESI-MS analysis. Dedication is made to Professor Michael P. Doyle on the occasion of his retirement.

REFERENCES

- (1). Weissermel K; Arpe H-J Alcohols. Industrial Organic Chemistry, 4th ed.; Wiley-VCH: Hoboken, 2008; pp 193–215.
- (2). (a) Smith MBMarch's Advanced Organic Chemistry, 7th ed.; Wiley: New York, 2013.(b) Beller M; Seayad J; Tillack A; Jiao H Angew. Chem., Int. Ed 2004, 43, 3368–3398.
- (3). (a) Brown HC; Zweifel G A Stereospecific *cis*-Hydration of the Double Bond in Cyclic Derivatives. J. Am. Chem. Soc 1959, 81, 247–247.(b) Brown HC; Rao BCS A New Technique for the Conversion of Olefins into Organoboranes and Related Alcohols. J. Am. Chem. Soc 1956, 78, 5694–5695.
- (4). (a) Noweck K; Grafahrend WFatty Alcohols. In Ullmann's Encyclopedia of Industrial Chemistry.; Wiley-VCH: Weinheim, Germany, 2006; Vol. 14, pp117–141.(b) Eilbracht P; Bäracker L; Buss C; Hollmann C; Kitsos-Rzychon BE; Kranemann CL; Rische T; Roggenbuck R; Schmidt A Tandem Reaction Sequences under Hydroformylation Conditions: New Synthetic Applications of Transition Metal Catalysis. Chem. Rev 1999, 99, 3329–3366. [PubMed: 11749518] (c) Franke R; Selent D; Börner A Applied Hydroformylation. Chem. Rev 2012, 112, 5675–5732. [PubMed: 22937803] (d) Torres GM; Frauenlob R; Franke R; Börner A Production of Alcohols via Hydroformylation. Catal. Sci. Technol 2015, 5, 34–54.(e) Diab L; Šmejkal T; Geier J; Breit B Supramolecular Catalyst for Aldehyde Hydrogenation and Tandem Hydroformylation–Hydrogenation. Angew. Chem., Int. Ed 2009, 48, 8022–8026.(f) Takahashi K; Yamashita M; Ichihara T; Nakano K; Nozaki K High-Yielding Tandem Hydroformylation/Hydrogenation of a Terminal Olefin to Produce a Linear Alcohol Using a Rh/Ru Dual Catalyst System. Angew. Chem., Int. Ed 2010, 49, 4488–4490.(g) Takahashi K; Yamashita M; Nozaki K Tandem Hydroformylation/Hydrogenation of Alkenes to Normal Alcohols Using Rh/Ru Dual Catalyst or Ru Single Component Catalyst. J. Am. Chem. Soc 2012, 134, 18746–18757. [PubMed: 23116366] (h) Wu L; Fleischer I; Jackstell R; Profir I; Franke R; Beller M Ruthenium-Catalyzed Hydroformylation/Reduction of Olefins to Alcohols: Extending the Scope to Internal Alkenes. J. Am. Chem. Soc 2013, 135, 14306–14312. [PubMed: 23987582]
- (5). (a) Yao C; Dahmen T; Gansauer A; Norton J *Anti*-Markovnikov Alcohols via Epoxide Hydrogenation through Cooperative Catalysis. Science 2019, 364, 764–767. [PubMed: 31123133] (b) Liu W; Li W; Spannenberg A; Junge K; Beller M Iron-Catalysed Regioselective Hydrogenation of Terminal Epoxides to Alcohols under Mild Conditions. Nat. Catal 2019, 2, 523–528.(c) Parasram M; Shields BJ; Ahmad O; Knauber T; Doyle AG Regioselective Cross-Electrophile Coupling of Epoxides and (Hetero)aryl Iodides via Ni/Ti/Photoredox Catalysis. ACS Catal. 2020, 10, 5821–5827. [PubMed: 32747870] (d) Funk BE; Pauze M; Lu Y-C; Moser AJ; Wolf G; West JG Vitamin B₁₂ and Hydrogen Atom Transfer Cooperative Catalysis as a

Hydride Nucleophile Mimic in Epoxide Ring Opening. *Cell Rep. Phys. Sci* 2023, 4, No. 101372. [PubMed: 37235063]

- (6). (a) Hintermann L. Recent Developments in Metal-Catalyzed Additions of Oxygen Nucleophiles to Alkenes and Alkynes. In *C-X Bond Formation*; Vigalok A, Ed.; Topics in Organometallic Chemistry; Springer: Berlin, 2010; Vol. 31, pp 123–155. (b) Margrey KA; Nicewicz DA A General Approach to Catalytic Alkene Anti-Markovnikov Hydrofunctionalization Reactions via Acridinium Photoredox Catalysis. *Acc. Chem. Res* 2016, 49, 1997–2006. [PubMed: 27588818]
- (7). Dong G; Teo P; Wickens ZK; Grubbs RH Primary Alcohols from Terminal Olefins: Formal *Anti*-Markovnikov Hydration via Triple Relay Catalysis. *Science* 2011, 333, 1609–1612. [PubMed: 21921194]
- (8). Hu X; Zhang G; Bu F; Lei A Visible-Light-Mediated *Anti*-Markovnikov Hydration of Olefins. *ACS Catal.* 2017, 7, 1432–1437.
- (9). (a) Pratley C; Fenner S; Murphy JA Nitrogen-Centered Radicals in Functionalization of sp² Systems: Generation, Reactivity, and Applications in Synthesis. *Chem. Rev* 2022, 122, 8181–8260. [PubMed: 35285636] (b) Musacchio AJ; Lainhart BC; Zhang X; Naguib SG; Sherwood TC; Knowles RR Catalytic Intermolecular Hydroaminations of Unactivated Olefins with Secondary Alkyl Amines. *Science* 2017, 355, 727–730. [PubMed: 28209894] (c) Lardy SW; Schmidt VA Intermolecular Radical Mediated Anti-Markovnikov Alkene Hydroamination Using N-Hydroxyphthalimide. *J. Am. Chem. Soc* 2018, 140, 12318–12322. [PubMed: 30192532] (d) Miller DC; Ganley JM; Musacchio AJ; Sherwood TC; Ewing WR; Knowles RR Anti-Markovnikov Hydroamination of Unactivated Alkenes with Primary Alkyl Amines. *J. Am. Chem. Soc* 2019, 141, 16590–16594. [PubMed: 31603324] (e) Park S; Jeong J; Fujita K.-i.; Yamamoto A; Yoshida H Anti-Markovnikov Hydroamination of Alkenes with Aqueous Ammonia by Metal-Loaded Titanium Oxide Photocatalyst. *J. Am. Chem. Soc* 2020, 142, 12708–12714. [PubMed: 32568530] (f) Lindner H; Amberg WM; Carreira EM Iron-Mediated Photochemical Anti-Markovnikov Hydroazidation of Unactivated Olefins. *J. Am. Chem. Soc* 2023, 145, 22347–22353. [PubMed: 37811819]
- (10). (a) Fairbanks BD; Macdougall LJ; Mavila S; Sinha J; Kirkpatrick BE; Anseth KS; Bowman CN Photoclick Chemistry: A Bright Idea. *Chem. Rev* 2021, 121, 6915–6990. [PubMed: 33835796] (b) Beletskaya IP; Ananikov VP Transition-Metal-Catalyzed C—S, C—Se, and C—Te Bond Formations via Cross-Coupling and Atom-Economic Addition Reactions. Achievements and Challenges. *Chem. Rev* 2022, 122, 16110–16293. [PubMed: 36112510] (c) Tyson EL; Ament MS; Yoon TP Transition Metal Photoredox Catalysis of Radical Thiol-Ene Reactions. *J. Org. Chem* 2013, 78, 2046–2050. [PubMed: 23094660] (d) Hell SM; Meyer CF; Misale A; Sap JBI; Christensen KE; Willis MC; Trabanco AA; Gouverneur V Hydrosulfonylation of Alkenes with Sulfonyl Chlorides under Visible Light Activation. *Angew. Chem., Int. Ed* 2020, 59, 11620–11626. (e) Renzi P; Azzi E; Ascensio S; Parisotto S; Sordello F; Pellegrino F; Ghigo G; Deagostino A Inexpensive and Bench Stable Diarylmethylum Tetrafluoroborates as Organocatalysts in the Light Mediated Hydrosulfonylation of Unactivated Alkenes. *Chem. Sci* 2023, 14, 2721–2734. [PubMed: 36908942] (f) Song Y; Li C; Hu X; Zhang H; Mao Y; Wang X; Wang C; Hu L; Yan J Light-promoted Photocatalyst-free and Redox-neutral Hydrosulfonylation of Unactivated Alkenes Using Sulfinic Acid. *Green Chem.* 2024, 26, 6578.
- (11). (a) Kharasch MS; Mayo FR The Peroxide Effect in the Addition of Reagents to Unsaturated Compounds. I. The Addition of Hydrogen Bromide to Allyl Bromide. *J. Am. Chem. Soc* 1933, 55, 2468–2496. (b) Kim J; Sun X; van der Worp BA; Ritter T Anti-Markovnikov Hydrochlorination and Hydronitroxylation of α -Olefins via Visible-light Photocatalysis. *Nat. Catal* 2023, 6, 196–203.
- (12). Lai S-Q; Wei B-Y; Wang J-W; Yu W; Han B Photocatalytic Anti-Markovnikov Radical Hydro- and Aminoxygenation of Unactivated Alkenes Tuned by Ketoxime Carbonates. *Angew. Chem., Int. Ed* 2021, 60, 21997–22003.
- (13). Leng L; Ready JM Hydroesterification and Difunctionalization of Olefins with N-Hydroxyphthalimide Esters. *ACS Catal.* 2021, 11, 13714–13720. [PubMed: 35982833]
- (14). (a) Quach L; Dutta S; Pflüger PM; Sandfort F; Bellotti P; Glorius F Visible-Light-Initiated Hydrooxygenation of Unactivated Alkenes—A Strategy for Anti-Markovnikov Hydrofunctionalization. *ACS Catal.* 2022, 12, 2499–2504. (b) Tan G; Paulus F; Rentería-Gómez Á; Lalisce RF; Daniliuc CG; Gutierrez O; Glorius F Highly Selective Radical Relay 1,4-

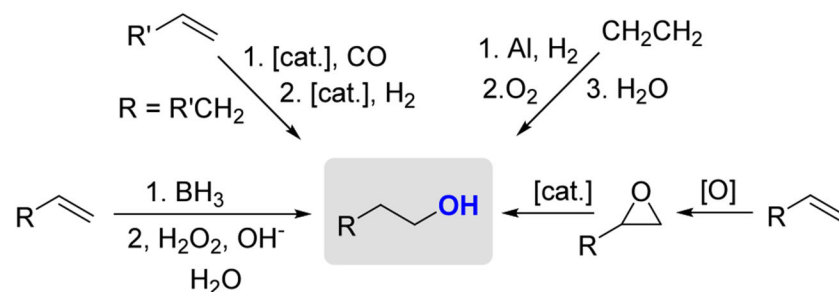
Oxyimination of Two Electronically Differentiated Olefins. *J. Am. Chem. Soc.* 2022, 144, 21664–21673. [PubMed: 36383483]

- (15). (a) Wang B; Ascenzi Pettenuzzo C; Singh J; McCabe GE; Clark L; Young R; Pu J; Deng Y Photoinduced Site-Selective Functionalization of Aliphatic C—H Bonds by Pyridine N-oxide Based HAT Catalysts. *ACS Catal.* 2022, 12, 10441–10448. (b) Schlegel M; Qian S; Nicewicz DA Aliphatic C—H Functionalization Using Pyridine N-Oxides as H-Atom Abstraction Agents. *ACS Catal.* 2022, 12, 10499–10505. [PubMed: 37727583] (c) Ciszewski ŁW; Gryko D Pyridine N-oxides as HAT Reagents for Photochemical C—H Functionalization of Electron-deficient Heteroarenes. *Chem. Commun* 2022, 58, 10576–10579. (d) Laze L; Quevedo-Flores B; Bosque I; Gonzalez-Gomez JC Alkanes in Minisci-Type Reaction under Photocatalytic Conditions with Hydrogen Evolution. *Org. Lett* 2023, 25, 8541–8546. [PubMed: 37819209] (e) Pang H; Liu G; Huang D; Zhu Y; Zhao X; Wang W; Xiang Y Embedding Hydrogen Atom Transfer Moieties in Covalent Organic Frameworks for Efficient Photocatalytic C—H Functionalization. *Angew. Chem., Int. Ed* 2023, 62, No. e202313520. (f) Xu J.-h.; Wu W.-b.; Wu J Photoinduced Divergent Alkylation/Acylation of Pyridine N-Oxides with Alkynes under Anaerobic and Aerobic Conditions. *Org. Lett* 2019, 21, 5321–5325. [PubMed: 31247751] (g) Deng Y; Zhang J; Bankhead B; Markham JP; Zeller M Photoinduced Oxidative Cyclopropanation of Ene-namides: Synthesis of 3-Aza[n.1.0]bicycles via Vinyl Radicals. *Chem. Commun* 2021, 57, 5254–5257. (h) Wang B; Singh J; Deng Y Photoredox-Catalyzed Divergent Radical Cascade Annulations of 1,6-Enynes via Pyridine N-Oxide-Promoted Vinyl Radical Generation. *Org. Lett* 2023, 25, 9219–9224. [PubMed: 38112553]
- (16). Roth HG; Romero NA; Nicewicz DA Experimental and Calculated Electrochemical Potentials of Common Organic Molecules for Applications to Single-Electron Redox Chemistry. *Synlett* 2016, 27, 714–723.
- (17). Zhou W; Miura T; Murakami M Photocatalyzed ortho-Alkylation of Pyridine N-Oxides through Alkene Cleavage. *Angew. Chem., Int. Ed* 2018, 57, 5139–5142.
- (18). These differential experimental observations from **1b** and **1d** are consistent with our DFT modeling of the first step in the reaction of 1-hexene with **1b/1d**. The *N*-oxy radical of **1b** favored alkene addition over allylic C-H abstraction by 1.3 kcal/mol, while the *N*-oxy radical of **1d** favored allylic C-H abstraction by 1.4 kcal/mol (See Supporting Information for details of these calculations). However, it must be noted that the chemoselectivity-determining step in these competing pathways most likely occurs after this initial engagement of the *N*-oxy radicals with the α -olefins.
- (19). Romero NA; Margrey KA; Tay NE; Nicewicz DA Site-selective Arene C-H Amination via Photoredox Catalysis. *Science* 2015, 349, 1326–1330. [PubMed: 26383949]
- (20). Deposition numbers 2355768 (14) contains the supplementary crystallographic data for this paper. These data can be obtained free of charge from The Cambridge Crystallographic Data Centre via www.ccdc.cam.ac.uk/datarequest/cif.
- (21). (a) Huang N; Luo J; Liao L; Zhao X Catalytic Enantioselective Aminative Difunctionalization of Alkenes. *J. Am. Chem. Soc.* 2024, 146, 7029–7038. [PubMed: 38425285] (b) Torregrosa-Chinillach A; Carral-Menoyo A; Gómez-Bengoia E; Chinchilla R Organocatalytic Enantioselective α -Nitrogenation of α,α -Disubstituted Aldehydes in the Absence of a Solvent. *J. Org. Chem* 2022, 87, 14507–14513. [PubMed: 36283071]
- (22). (a) Katritzky AR; Lunt E N-oxides and related compounds—XXXV: Reactions of N-alkoxy-pyridinium and -quinolinium cations with nucleophiles. *Tetrahedron* 1969, 25, 4291–4305. (b) Bauer L; Gardella LA The Chemistry of Pyridine. II. The Reaction of 1-Alkoxypicolinium Salts with Mercaptide and Thiophenoxide Ions. *J. Org. Chem* 1963, 28, 1323–1328.
- (23). (a) Lee DS; Soni VK; Cho EJ N—O Bond Activation by Energy Transfer Photocatalysis. *Acc. Chem. Res* 2022, 55 (17), 2526–2541. [PubMed: 35986693] (b) He F-S; Ye S; Wu J Recent Advances in Pyridinium Salts as Radical Reservoirs in Organic Synthesis. *ACS Catal.* 2019, 9 (10), 8943–8960. (c) Ma X; Dang H; Rose JA; Rablen P; Herzon SB Hydroheteroarylation of Unactivated Alkenes Using N-Methoxyheteroarene Salts. *J. Am. Chem. Soc.* 2017, 139 (16), 5998–6007. [PubMed: 28359149] (d) Das M; Zamani L; Bratcher C; Musacchio PZ Azolation of Benzylic C—H Bonds via Photoredox-Catalyzed Carbocation Generation. *J. Am. Chem. Soc.* 2023, 145 (7), 3861–3868. (e) Kim I; Park B; Kang G; Kim J; Jung H; Lee H; Baik M-H; Hong S Visible-Light-Induced Pyridylation of Remote C(sp³)—H Bonds by Radical Translocation of N-

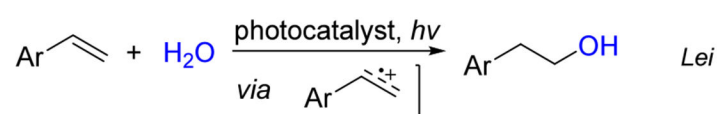
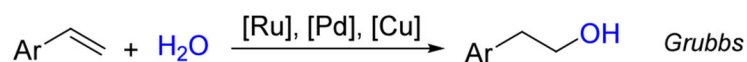
Alkoxyppyridinium Salts. *Angew. Chem., Int. Ed* 2018, 57 (47), 15517–15522.(f) Barthelemy A-L; Tuccio B; Magnier E; Dagousset G Alkoxy Radicals Generated under Photoredox Catalysis: A Strategy for anti-Markovnikov Alkoxylation Reactions. *Angew. Chem., Int. Ed* 2018, 57 (42), 13790–13794.(g) Bao X; Wang Q; Zhu J Dual Photoredox/Copper Catalysis for the Remote C(sp³)—H Functionalization of Alcohols and Alkyl Halides by N-Alkoxyppyridinium Salts. *Angew. Chem., Int. Ed* 2019, 58 (7), 2139–2143.

- (24). (a) Becke AD Density-functional thermochemistry. I. The effect of the exchange-only gradient correction. *J. Chem. Phys* 1992, 96, 2155–2160.(b) Hehre W; Ditchfield R; Stewart R; Pople J self-consistent molecular orbital methods. iv. use of Gaussian expansions of Slater-type orbitals. Extension to second-row molecules. *J. Chem. Phys* 1970, 52, 2769–2773.(c) Grimme S; Ehrlich S; Goerigk L Effect of the damping function in dispersion corrected density functional theory. *J. Comput. Chem* 2011, 32, 1456–1465. [PubMed: 21370243]
- (25). (a) Miertuš S; Scrocco E; Tomasi J Electrostatic interaction of a solute with a continuum. A direct utilization of AB initio molecular potentials for the prevision of solvent effects. *Chem. Phys* 1981, 55, 117–129.(b) Tomasi J; Mennucci B; Cammi R Quantum mechanical continuum solvation models. *Chem. Rev* 2005, 105, 2999–3094. [PubMed: 16092826]
- (26). Frisch MJ; Trucks GW; Schlegel HB; Scuseria GE; Robb MA; Cheeseman JR; Scalmani G; Barone V; Petersson GA; Nakatsuji H; Li X; Caricato M; Marenich AV; Bloino J; Janesko BG; Gomperts R; Mennucci B; Hratchian HP; Ortiz JV; Izmaylov AF; Sonnenberg JL; Williams; Ding F; Lipparini F; Egidi F; Goings J; Peng B; Petrone A; Henderson T; Ranasinghe D; Zakrzewski VG; Gao J; Rega N; Zheng G; Liang W; Hada M; Ehara M; Toyota K; Fukuda R; Hasegawa J; Ishida M; Nakajima T; Honda Y; Kitao O; Nakai H; Vreven T; Throssell K; Montgomery JA Jr.; Peralta JE; Ogliaro F; Bearpark MJ; Heyd JJ; Brothers EN; Kudin KN; Staroverov VN; Keith TA; Kobayashi R; Normand J; Raghavachari K; Rendell AP; Burant JC; Iyengar SS; Tomasi J; Cossi M; Millam JM; Klene M; Adamo C; Cammi R; Ochterski JW; Martin RL; Morokuma K; Farkas O; Foresman JB; Fox DJ *Gaussian 16* Rev. C.01.; Gaussian Inc., 2016.
- (27). See Supporting Information for full details of the SET thermodynamics calculations.
- (28). It must be noted that the corresponding transition state for the addition of 1b• to the electron-deficient benzalmalonitrile had a barrier of 3.7 kcal/mol, suggesting that 1b• is an electrophilic radical that selectively adds to more electron-rich alkenes.
- (29). We also modeled the displacement of pyridine N-oxide by attack of water (both with and without activation by trifluoroacetate) on Int1, Int2, and Int3 and found these TSs to have much higher barriers than TSSub. The full details of these calculations are in the Supporting Information.

A. Stepwise synthesis of primary alcohols



B. Catalytic synthesis of primary alcohols from alkenes



C. Catalytic regioselective hydroxygenation of alkenes

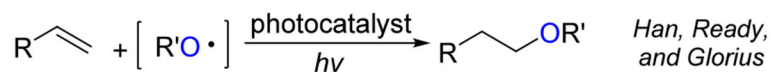


Figure 1. (A) Stepwise synthesis of primary alcohols. (B) Representative examples on catalytic synthesis of primary alcohols. (C) Photoredox catalyzed anti-Markovnikov hydroxygenation of unactivated olefins.

This Work: regioselective carbo- and amino-hydroxylation of unactivated α -olefins

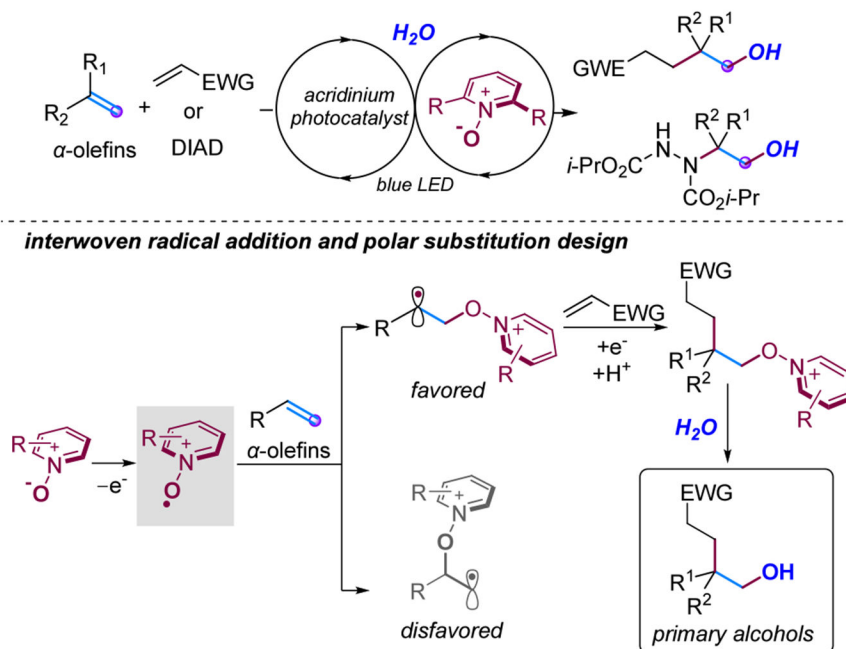


Figure 2.

This work: photoredox/pyridine N -oxide catalyzed regioselective carbohydroxylation and aminohydroxylation of α -olefins with water for the synthesis of primary alcohols.

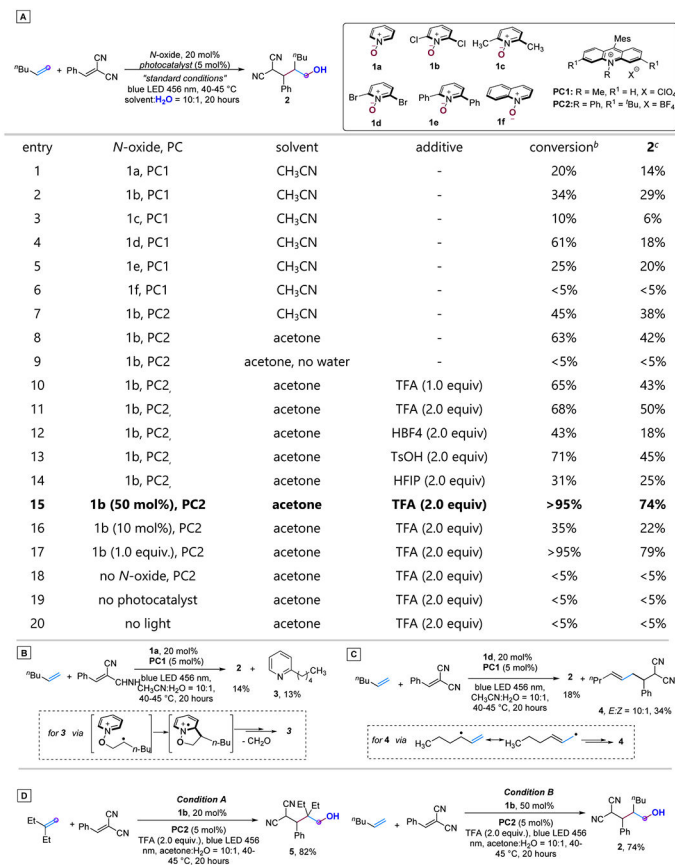


Figure 3. (A) Reaction Optimization. (B) Reaction of pyridine *N*-oxide **1a**. (C) Reaction of 2,6-dibromopyridine *N*-oxide **1d**. (D) Optimized conditions A and B. Reaction conditions: alkene (0.6 mmol, 3.0 equiv), benzaldehyde malononitrile (0.2 mmol, 1.0 equiv), 20 mol % of *N*-oxide, and 5 mol % of photocatalyst in solvent/H₂O = 10:1 (2.0 mL) under blue LED light ($\lambda_{\text{max}} = 456 \text{ nm}$, 34 W) for 20 h. ^bConversion of benzaldehyde malononitrile. ^cYields were determined by analysis of the ¹H NMR spectra of the reaction mixture using dibromomethane as an internal standard, and regioselectivity was determined by crude ¹H NMR analysis.

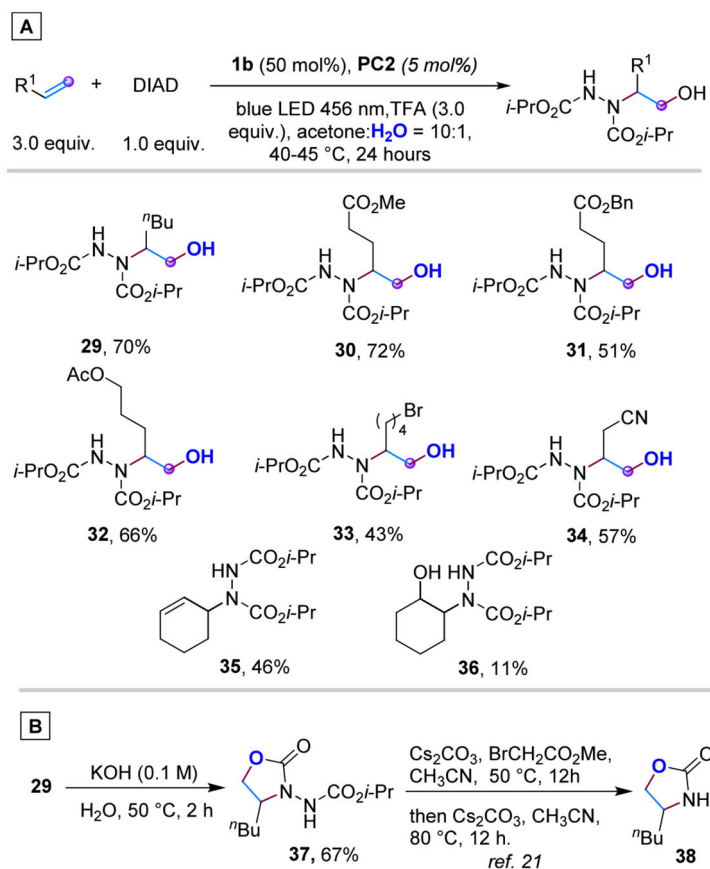


Figure 5. (A) Synthetic scope for photoredox/pyridine *N*-oxide catalyzed regioselective aminohydroxylation of α -olefins. (B) Derivatization of **29**. See the Supporting Information for full experimental details and conditions.

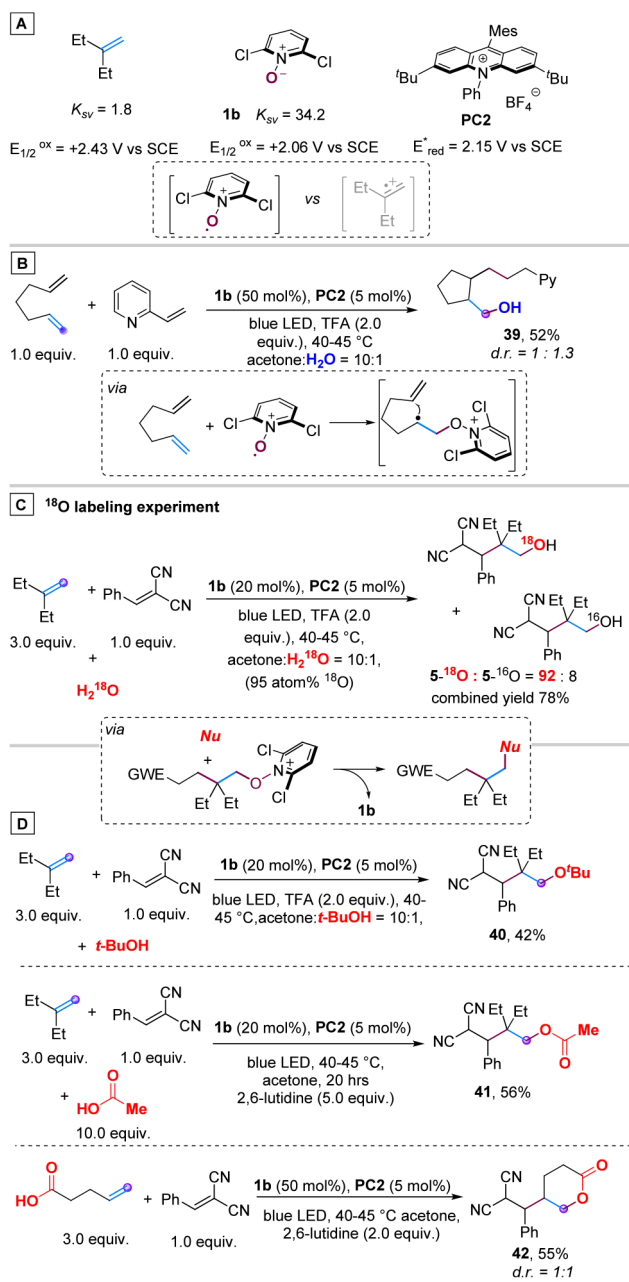


Figure 6. (A) Evidence for pyridine *N*-oxide (**1b**) as a reductive quencher. (B) Carbon radical trapping by intramolecular cyclization of 1,6-heptadiene. (C) ¹⁸O Labeling experiment. (D) Regioselective carboetherification and carboesterification.

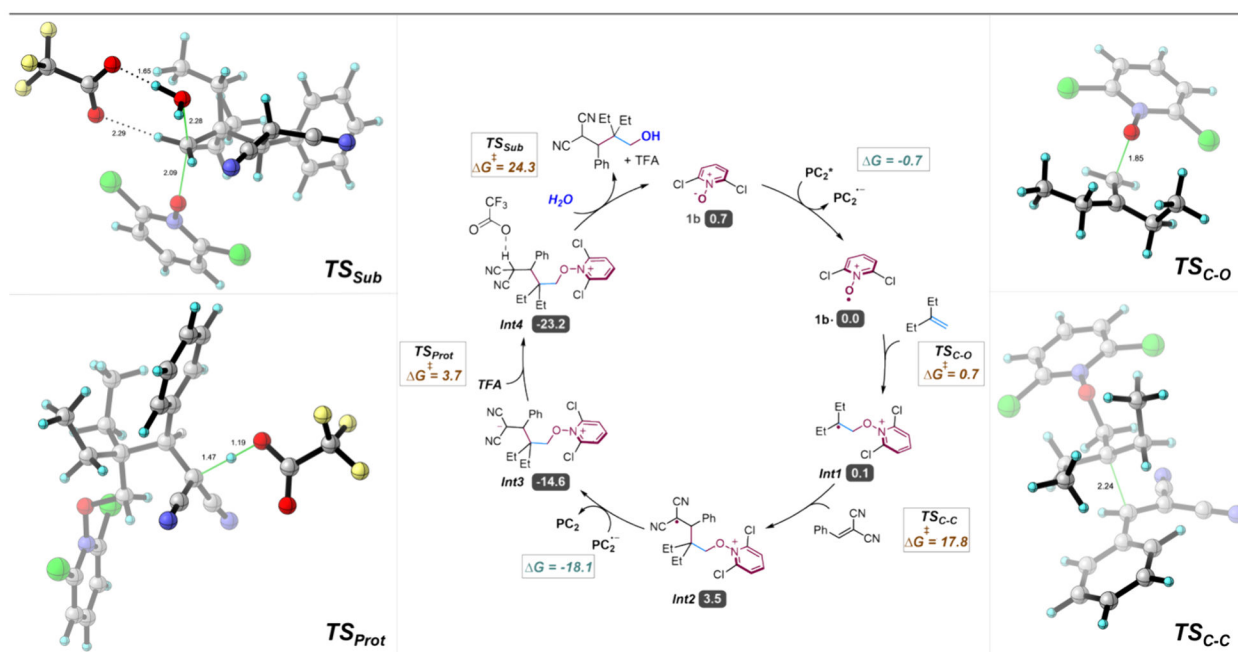


Figure 7. Most likely catalytic cycle for the photoredox/pyridine *N*-oxide catalyzed regioselective carbohydroxylation of 2-ethyl 1-butene and benzal malononitrile computed using B3LYP-D3(BJ)/6-31+G* PCM(acetone). Numbers under each structure represent the free energy (in kcal/mol) of that structure relative to the energy of the *N*-oxy radical of **1b** computed at 318 K. The ΔG values on the arrows represent the thermodynamics of the SET steps while the ΔG^\ddagger values correspond to the free energy barrier of the TS relative to the free energy of the preceding intermediate. All transition structures are rendered using CYLView 2.0 with key distances in angstroms (Å).